

Ultrasound-Engineered fabrication of immobilized molybdenum complex on Cross-Linked poly (Ionic Liquid) as a new acidic catalyst for the regioselective synthesis of pharmaceutical polysubstituted spiro compounds

Zahra Elyasi^a, Javad Safaei Ghomi^{a,b,*}, Gholam Reza Najafi^a

^a Department of Chemistry, Qom Branch, Islamic Azad University, Qom, Islamic Republic of Iran

^b Department of Organic Chemistry, Faculty of Chemistry, University of Kashan, Islamic Republic of Iran

ARTICLE INFO

Keywords:

Poly (ionic liquid)
Heterogeneous catalyst
Ultrasound
Molybdenum complex
Regioselective synthesis

ABSTRACT

A novel supported molybdenum complex on cross-linked poly (1-Aminopropyl-3-vinylimidazolium bromide) entrapped cobalt oxide nanoparticles has been successfully fabricated through two different procedures, i.e. ultrasound (US) irradiations (100 W, 40 kHz) and reflux. The efficiency of the two different methods was comparatively investigated on the fundamental properties of proposed catalyst using diverse characterization techniques. Based on the obtained results, the ultrasonication method provides controlled polymerization process; as a result, well connected polymeric network is formed. In addition, the use of ultrasound waves turned out to be able to increase the particles uniformity, specific surface area (from 79.19 to 223.83 m²/g), and the onset thermal degradation temperature (T_d) value (from 248 to 400 °C) of the prepared catalyst which intensifies the catalytic efficiency. Besides, US-treated catalyst demonstrated high chemical stability and maintained its cross-linked network after eight cycles recovery, while the cross-linked network of catalyst obtained under silent condition was completely disrupted. Furthermore, the ultrafast multi-step fabrication procedure was performed in less than 6 h under ultrasonic condition while a similar process promoted by a mechanical stirring method came to a conclusion after 5–6 days. Accordingly, the utility of the ultrasound irradiation was proved, and US-treated catalyst was applied for improved synthetic methodology of spiro 1,4-dihydropyridines and spiro pyranopyrazoles through different acidic active sites. Due to the significant synergistic influence between the proposed catalyst and US irradiation, a variety of novel and recognized mono-spiro compounds were fabricated at room temperature in high regioselectivity.

1. Introduction

As one of the effective and greenest techniques, sonochemistry is interesting in the synthesis of nanomaterials and various bulks [1,2]. Ultrasound-assisted synthesis has been widely used due to its mechanical, physical, or chemical effects on the process. It is obvious that exposure of nanomaterials, various bulk, and polymer solutions to low-frequency (20–100 kHz), high-intensity (10–1000 W/cm⁻²) ultrasound induces great changes to their textural and morphological properties such as particle size, viscosity properties, gelling property, thermal stability, and biological activity [3]. Moreover, the synthesis of substances under ultrasonic condition not only requires fewer catalysts and

solvents, but also meets the ecological requirements more efficiently [4]. Although the interaction between ultrasound irradiation and molecules is not direct, the energy of the ultrasound waves can cause acoustic cavitation, which provokes different physical and chemical effects. During this process, the implosion of the bubbles leads to the release of a large amount of mechanical and thermal energy without any significant change in the reaction medium (in terms of pressure and temperature) [5]. Consequently, the use of ultrasonic irradiation accelerates an organic transformation at the synthesis pathway, and it has been extensively employed in recent decades according to its specific properties.

2-Oxindoles, especially those spiro-fused to other cyclic frameworks,

* Corresponding author at: Department of Chemistry, Qom Branch, Islamic Azad University, Post Box: 37491-13191, Qom, Islamic Republic of Iran; Department of Organic Chemistry, Faculty of Chemistry, University of Kashan, Islamic Republic of Iran.

E-mail address: safaei@kashanu.ac.ir (J.S. Ghomi).

<https://doi.org/10.1016/j.ultsonch.2021.105614>

Received 12 March 2021; Received in revised form 17 May 2021; Accepted 27 May 2021

Available online 1 June 2021

1350-4177/© 2021 Published by Elsevier B.V. This is an open access article under the CC BY-NC-ND license (<http://creativecommons.org/licenses/by-nc-nd/4.0/>).

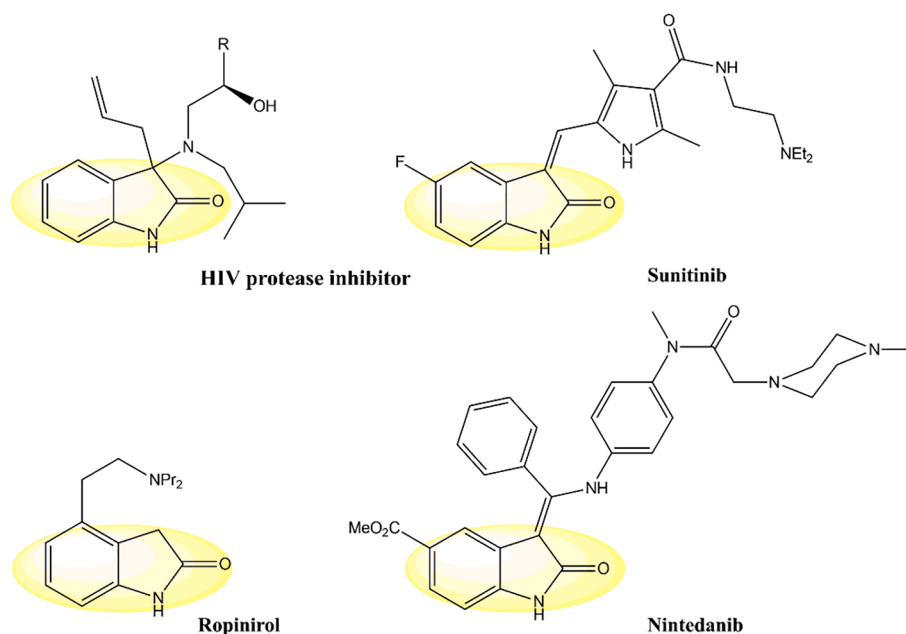


Fig. 1. Biologically active 2-Oxindoles.

are structural motifs in organic chemistry due to their widespread bioavailability and pharmacological applications such as HIV protease inhibitor [6], anti-inflammatory [7], anti-cancer [8], antimicrobial [9], anti-hypertensive [10], and anti-diabetic [11]. Among various drugs with a 2-oxindole core that have already been developed, only four marketed molecules; namely, Sunitinib proposed in pancreatic neuroendocrine tumors, Ropinirol utilized for Parkinson's disease treatment, Nintedanib known as a drug against idiopathic pulmonary fibrosis, and HIV protease inhibitor have appeared in Fig. 1. Both functionalized spiro 1,4-dihydropyridines and spiro pyranopyrazoles are important branches of biologically active organic compounds [12,13]. Recently, owing to their great biological properties, some straightforward methods have been reported for their preparation using one-pot four-component reactions. However, some of these protocols suffer from limitations such as prolonged catalyst preparation, elevated temperature, and using hazardous and expensive reagents besides byproducts. It is believed that an effective general catalytic process for synthesizing both spiro 1,4-dihydropyridines and spiro pyranopyrazoles can be greatly promising and strongly desired.

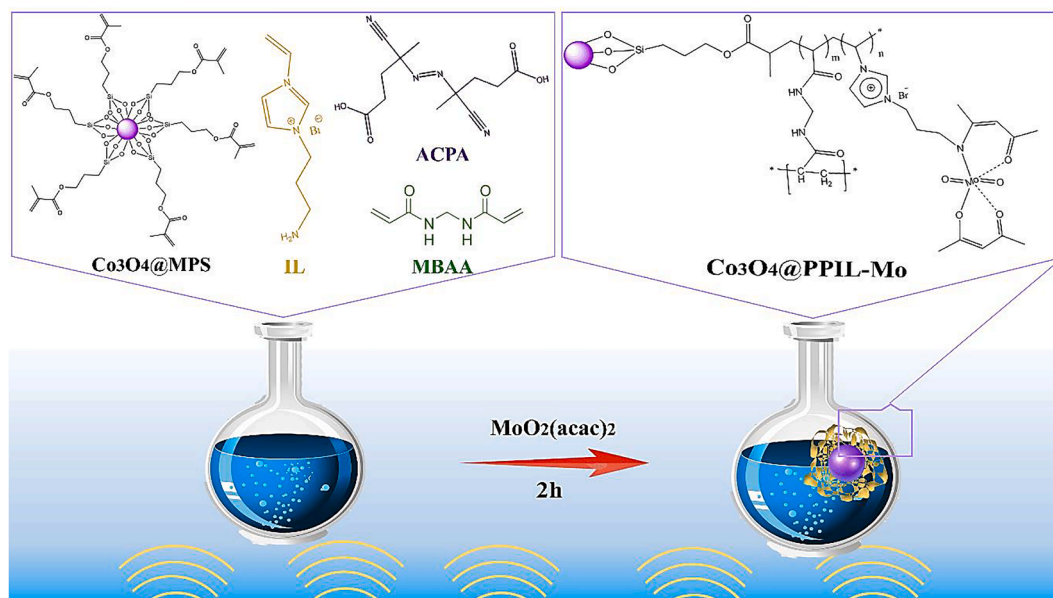
In recent years, ionic liquids (ILs) have been increasingly taken into consideration due to the fact that they can not only improve the catalytic activity, but also stabilize the reaction catalytic species [14–16]. However, some properties like homogeneity, high viscosity, and both leakage issue of ionic liquids limit their extensive use. To overcome these problems, ILs are generally supported by various components (polymers, metal oxides, silica, etc.) to obtain heterogeneous catalysts [17,18]. However, most IL-based catalysts need harsh conditions (high pressure/temperature) due to lack of active sites. Poly ionic liquids (PILs) or ionic liquid (IL) polymers are an emerging class of charged polymers having repeating units of polymerizable ionic moieties. They possess interesting properties of both conventional polymers (such as stiffness, tunable macromolecular structure, and mechanical strength) and those of the ILs (such as electrical conductivity, high thermal and chemical stability, and wide electrochemical potential window) [19–22]. Satisfying results in great molecular yields and weight are obtained while an oil-soluble radical initiator like Azobisisobutyronitrile (AIBN) with a traditional heating technology is used for radical polymerization. Although this technique is suffering from lack of control on the polymers' physico-chemical attributes, employing a water-soluble initiator as 4,4' Azobis (4-cyanopentanoic acid) can be considered a prominent solution to this

limitation [23,24]. Furthermore, transition metal complexes have also received increasing attention in the field of catalysis, and there are many reports about their catalytic utilization. These transition metal complexes, which are often in nano size, are immobilized on various supports to provide higher activity [25–27]. Although reported catalysts are effective, each of them has some disadvantages such as low loading, long reaction time, and harsh reaction condition. In general, designing and preparing a new efficient catalyst with high stability, selectivity, and recyclability is challenging in both industry and laboratory. To this end, we can claim that supported molybdenum on cross-linked PIL can be considered a smart way to overcome these problems due to the numerous functionalities that can be linked to it. It is worth noting that the immobilization of Mo (VI) Schiff base complexes into cross-linked poly ionic liquids has not previously been reported, either. In this regard, a fast and green method for the synthesis of scalable molybdenum Schiff base complex immobilized on porous poly ionic liquid (PPIL) framework is proposed and its efficiency in catalyzed synthesis of spiro-pyranopyrazoles and spiro-1,4-dihydropyridines is also explored. We develop polycyclic heterocycle framework by combining pyran, pyrazole, and spiro-oxindole motifs under mild condition. The proposed process highly complements the aims of green chemistry, and shows massive benefits both in industry and in academia.

2. Experimental

2.1. Materials

All chemicals grades were purchased from Merck and Scharlau in excellent purity. Melting point (m.p) was carried out by Electro-Thermal 9200, and Fourier transform infrared (FT-IR) spectroscopy was operated by Nicolet Magna-550 spectrometer (KBr pellets). ^1H and ^{13}C nuclear magnetic resonance (NMR) spectroscopy were obtained by Bruker at 300 and 75 MHz, respectively (in DMSO, internal reference: TMS). Philips-X'pertpro, an X-ray diffractometer utilizing Ni-filtered Cu K α radiation was employed for investigating X-ray diffraction (XRD) analysis, the particle size and morphological engineering were investigated by scanning electron microscopy (model: LEO-1455VP). A transmission electron microscope (TEM, Philips EM208S) was applied for the in-depth examination of morphology. The compositional analysis was done by Energy-dispersive X-ray (EDX, Kevex, Delta Class I).



Scheme 1. Synthetic route to obtain the $\text{Co}_3\text{O}_4\text{@PPIL-Mo}$ under ultrasound irradiation.

2.2. Synthesis of vinyl functionalized Co_3O_4 NPs

Co_3O_4 NPs were synthesized through chemical co-precipitation method according to our previous literature [28]. In short, 8.60 g of Cobalt (II) nitrate was dispersed in EtOH (100 ml) for about 30 min. Thereafter, 2.14 g of oxalic acid was slowly added and the solution was stirred for 1 h at 45 °C. Finally, the acquired precipitate was calcined for 2 h at 400 °C. The vinyl functionalized Co_3O_4 NPs were obtained via mixing NPs (1 g) and 3-(trimethoxysilyl) propylmethacrylate (MPS) (10 mmol) in EtOH under ultrasound condition (about 2 h). The same preparation method was carried out for 24 h under reflux condition according to the reported work [29]. Finally, to separate the MPS, coated $\text{Co}_3\text{O}_4\text{@MPS}$ was separated by centrifugation (6000 rpm, 5 min) and washed with EtOH to eliminate the unreacted compounds.

2.3. Fabrication of PPIL composite

Polymerization of aminopropyl-3-vinylimidazolium bromide [AVIM]Br (IL), induced by ACPA in the H_2O to form the porous ionic liquid network, was conducted. Ionic liquid was prepared according to our previous reported protocol [29]. Typically, vinyl functionalized Co_3O_4 NPs (0.5 g), (IL) (0.005 mol, 0.45 g), and crosslinker (N,N'-Methylenebis acrylamide) were dissolved into 10 ml deionized water and then submitted to an ultrasonic agitation for 15 min. In continuation, ACPA (1% mol, 0.029 g) was added as a water soluble initiator, and the mixture was sonicated about 1 h (refluxed for 8 h). The obtained powder was collected and treated subsequently by a drying approach to obtain $\text{Co}_3\text{O}_4\text{@PPILs}$ with unique textural properties. The probable mechanism of the precipitation polymerization process is shown in Scheme 1. The ACPA was decomposed by US irradiations and formed corresponding radicals through releasing nitrogen gas that abstracted electron from one of the terminal vinyl functional groups existing in $\text{Co}_3\text{O}_4\text{@MPS}$, and IL to produce the corresponding macro initiators. Mentioned macro radicals start IL grafting onto the $\text{Co}_3\text{O}_4\text{@MPS}$ leading to graft polymerization in the presence of the MBA, and finally, polymeric network is obtained

2.4. Fabrication of PPIL-Mo composite

The prepared poly ionic liquid was subjected to a complexation reaction. The obtained PIL (0.5 g) was ultrasonically dispersed in ethanol

(20 ml). Then bis (acetylacetonato) dioxomolybdenum (1 mmol) was added to the reaction mixture and submitted to ultrasonic agitation about 2 h (heated for 24 h at 60 °C). The final product was separated, washed several times with EtOH/ H_2O , and then dried in a vacuum oven and sieved.

2.5. Typical procedure for the synthesis of mono-spiro derivatives

Typically, isatins (1 mmol), activated methylene compounds (1.0 mmol), dimethyl acetylene dicarboxylate (DMAD), amine components (hydrate hydrazine, phenyl hydrazine, and aromatic amines), ultrasound treated catalyst (10 mol%), and water (5 ml), as a green solvent, were sonicated (ultrasonic bath) at room temperature or irradiated in a microwave oven at 200 W for an appropriate length of time as indicated in Tables 3 and 4. The reaction completion was checked by thin layer chromatography technique, and then the heterogeneous catalyst was separated. As the last step of multicomponent reaction, the crude precipitate was recrystallized from ethanol to obtain a pure product. All products were characterized by melting point (m.p.), ^1H NMR, ^{13}C NMR, FTIR, and elemental microanalysis. The spectral data of all compounds are provided in Supplementary Information.

2.6. Spectral data of new compounds

Methyl-6'-amino-5,7-dichloro-5'-cyano-2-oxo-2'H-spiro[indoline-3,4'-pyrano[2,3c]pyrazole]-3'-carboxylate (5f): White solid, m.p. > 300 °C. IR (KBr) ν : 3426, 3275, 3251, 2955, 2275, 1782, 1736, 1660, 1537, 1446, 1200, 1086, 920, 768 cm^{-1} ; ^1H NMR (300 MHz, DMSO-d_6) δ : 12.24 (s, 1H, NH), 10.55 (s, 1H, NH), 7.17 (s, 2H, NH_2), 6.98 (s, 1ArH), 6.88 (s, 1ArH), 4.09 (s, 3H, OMe); ^{13}C NMR (75 MHz, DMSO-d_6) δ : 182.5, 170.0, 158.0, 155.7, 144.2, 142.8, 127.2, 122.1, 118.7, 118.0, 113.9, 107.7, 103.4, 70.8, 28.3. Anal. calcd for $\text{C}_{16}\text{H}_9\text{Cl}_2\text{N}_5\text{O}_4$: C 47.31, H 2.23, N 17.24; found C 47.34, H 2.22, N 17.23.

Methyl-6'-amino-5,7-dichloro-5'-cyano-2-oxo-1'-phenyl-1'H-spiro[indoline-3,4'-pyrano[2,3c]pyrazole]-3'-carboxylate (5l): pink solid, mp > 300 °C; IR (KBr) ν : 3392, 3230, 3022, 2955, 2173, 1782, 1731, 1665, 1585, 1489, 1408, 1292, 1215, 1095, 937, 829, 779 cm^{-1} ; ^1H NMR (300 MHz, DMSO-d_6) δ : 10.40 (s, 1H, NH), 7.72–6.54 (m, 7 ArH, and NH_2), 3.37 (s, 3H, Me); ^{13}C NMR (75 MHz, DMSO-d_6) δ : 179.0, 167.4, 152.1, 151.9, 149.2, 142.0, 134.1, 133.7, 130.1, 124.0, 123.2, 121.7, 121.0, 118.3, 117.0, 107.3, 72.25, 35.92. Anal. Calcd. for $\text{C}_{22}\text{H}_{13}\text{Cl}_2\text{N}_5\text{O}_4$: C,

Table 1

Comparison of the experimental conditions under US irradiation and classical heating method.

Entry	Procedure	Condition	Time (h)	solvent	Ref.
1	Synthesis of [AVIM] Br	Δ	>24	acetonitrile	[31]
		US	less than 1	–	This work
2	Synthesis of NP@MPS	Δ	24–48	EtOH	[32]
		US	2	–	This work
3	Polymerization process	Δ	6–12	MeOH	[32]
		US	1	H ₂ O	This work
4	Immobilization of Mo (VI)	Δ	24–48	MeOH	[33]
		US	2	EtOH	This work

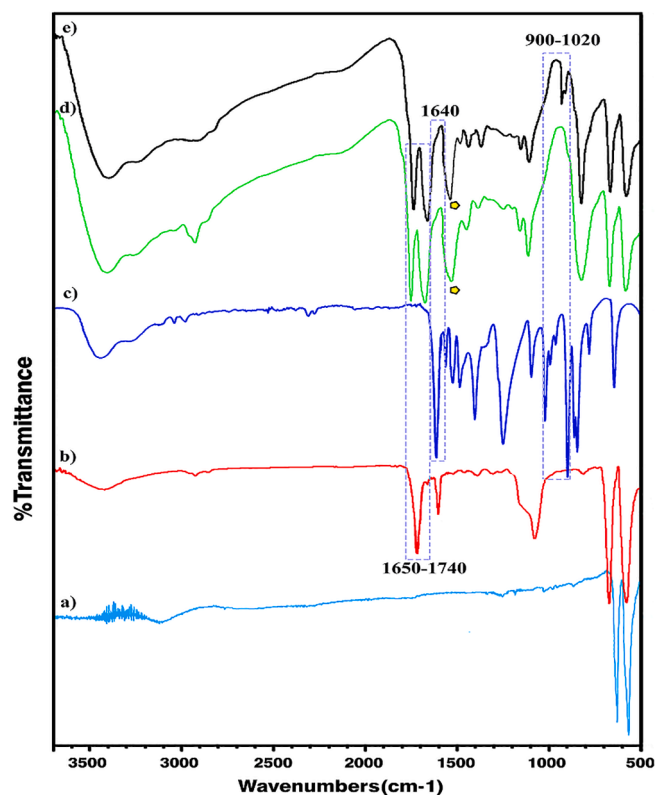


Fig. 2. FT-IR spectra of a) Co_3O_4 NPs, b) Co_3O_4 @MPS, c) IL monomers, d) Co_3O_4 @PPIL, and e) Desired Co_3O_4 @PPIL-Mo obtained from reflux conditions.

54.79; H, 2.72; N, 14.07; Found: C, 54.78; H, 2.71; N, 14.07.

3. Results and discussion

3.1. Characterization of Co_3O_4 @PPIL-Mo composite

Demonstrating the suitable conditions for nanoparticles' surfaces is considered one of their most significant alterations [30]. As a matter of fact, magnetic behavior of Fe_3O_4 NPs can enhance their significance because they are commonly absorbed into the magnet during the stirring. As a result, magnetic NPs cannot be efficiently dispersed. Therefore, not only are their surfaces not effectively functionalized, but also their polymerization flow is interrupted. Subsequently, more extended intense conditions must be applied to degrade polymer chains and core structure. To this end, the paramagnetic Co_3O_4 NPs were selected and polymerization of ionic monomers initiated and controlled by ultrasonic agitation. In this research, the performance of ultrasonic-assisted

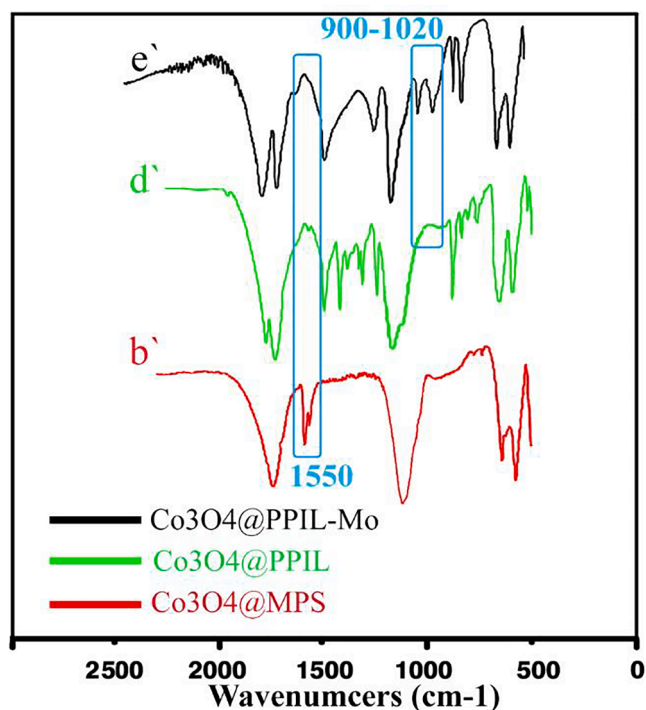


Fig. 3. FT-IR spectra of b') Co_3O_4 @MPS, d') Co_3O_4 @PPIL, and e') desired Co_3O_4 @PPIL-Mo obtained from US irradiations.

reaction is compared with a conventional heating method to achieve the most efficient condition for the fabrication of Co_3O_4 @PPIL-Mo. Furthermore, the synergistic catalytic effect is investigated between the prepared catalyst and the ultrasonic irradiation for the synthesis of mono-spiro derivatives. In addition, sonochemical one-pot multicomponent reactions were compared with the microwave-assisted reactions in details.

Firstly, Co_3O_4 NPs were prepared and sonochemically coated by silica network (MPS) for the first time. In the following, the monomeric IL was synthesized via quaternization of N-vinylimidazole with 3-bromopropylamine hydrobromide under ultrasound irradiation. We also introduce a straightforward method for controlled radical polymerization of silica-coated nanoparticles, ionic monomers, and MBAA as cross-linking agent via ultrasonic radiations. The proposed approach provides an excellent dispersion polymerization process by choosing a water-soluble initiator. Finally, sonochemical immobilization of molybdenum was carried out as the main active sites for catalytic performance.

With the aim of highlighting the efficiency of the proposed multi-step protocol, a comprehensive comparative study was done (Table 1). At first, the choice of ultrasound method is an intelligent tactic from various aspects (such as economic, environmental, practicality, etc.). Acoustic cavitation causes a special interaction of matter and energy, and ultrasonic radiation of liquids provides high energy chemical transformations to occur (especially, the reactions involving free radicals). Accordingly, these pluses will cause energy and time savings. All of these steps were performed in less than 6 h under ultrasonic condition while similar reported reactions promoted by a mechanical stirring method resulted in more time. Furthermore, in order to move to more sustainable methodologies, green and less hazardous solvents were replaced and some steps were carried out under solvent-free conditions.

The FT-IR spectroscopy study of the NPs, vinyl functionalized NPs, [AVIM]Br, Co_3O_4 @PPIL, and Co_3O_4 @PPIL-Mo was carried out to achieve more precise information. As illustrated in Fig. 2a, the peaks at 575 and 655 cm^{-1} are related to the spinel Co_3O_4 characteristic peaks [34]. Peaks at 1100, 1550, and 1740 cm^{-1} not only confirm successful coating of MPS, but are also related to Si-O, C = C, and carbonyl stretching

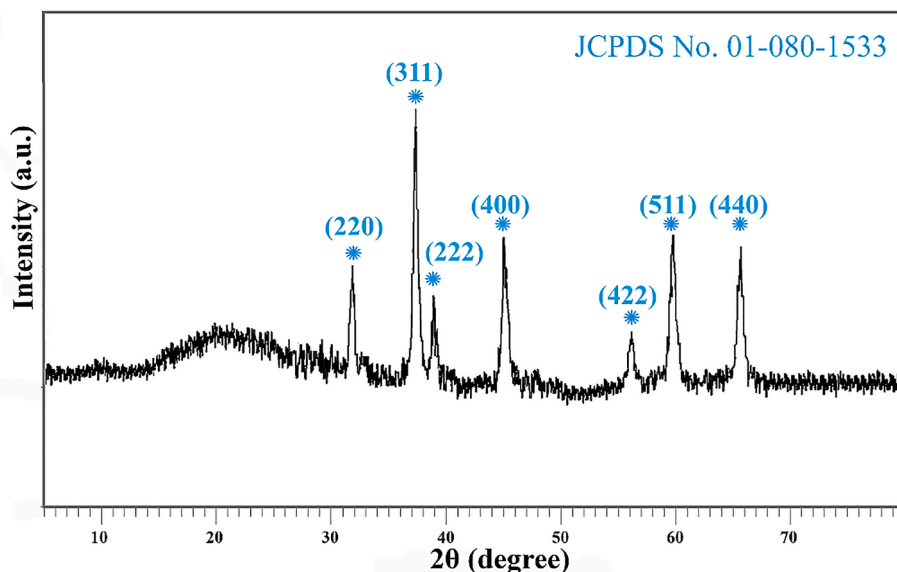


Fig. 4. XRD patterns of the US-treated Co_3O_4 @PPIL-Mo.

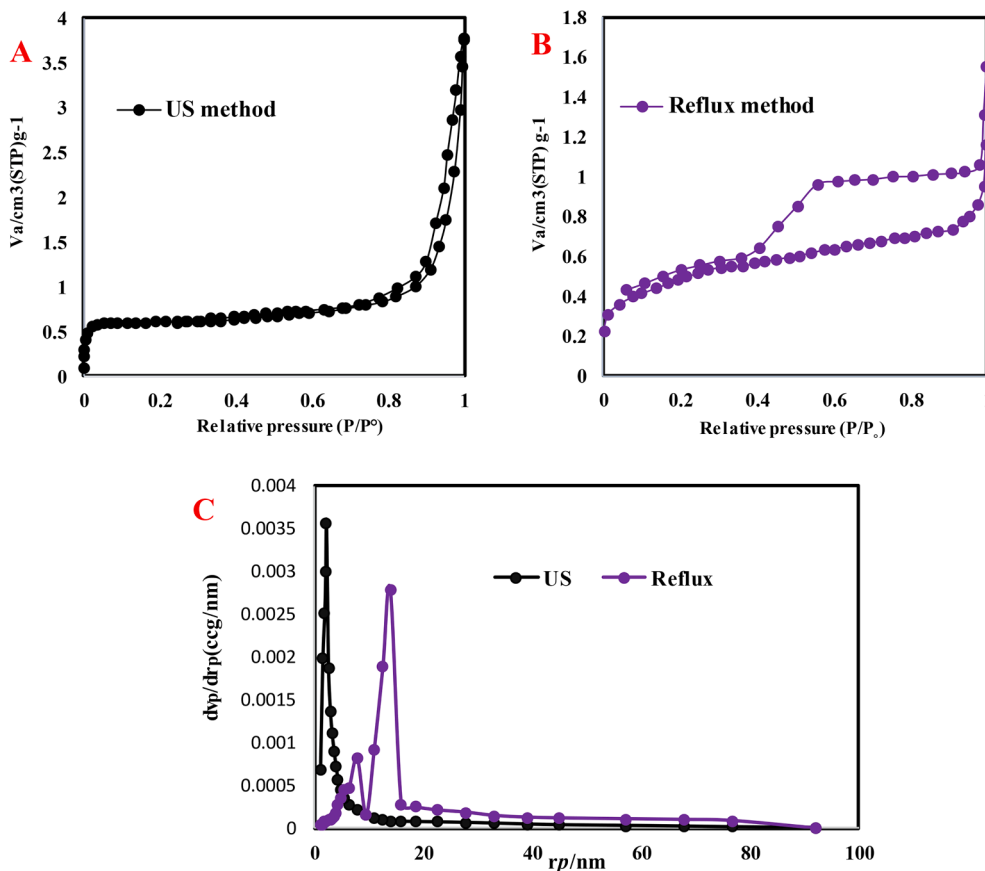


Fig. 5. A, B) N_2 adsorption-desorption isotherms and C) pore size distributions of Co_3O_4 @PPIL-Mo obtained from two different methods.

vibrations, respectively (Fig. 2b). As depicted in (Fig. 2c), vinyl group's stretching vibration appears at 1648 cm^{-1} . Moreover, bending vibration of the imidazole motif is emerged at $932\text{--}1020\text{ cm}^{-1}$. Nonetheless, these introduced peaks are not observed in the PIL spectrum, which confirms the polymerization (Fig. 2d). Unfortunately, the presence of $\text{C}=\text{C}$ MPS peak (1550) reveals incomplete polymerization process under reflux condition. $\text{N}-\text{C}-\text{N}$ characteristic peaks at 660 and 1228 cm^{-1} [35] are

preserved in the spectrum after the polymerization process (Fig. 2d). The strong absorbance band observed at 1670 cm^{-1} belongs to the characteristic peak of amide $\text{C}=\text{O}$ (Fig. 2d). Finally, incomplete and the uncontrolled polymerization process led to partial complexation of Mo (VI). The FT-IR spectrum of the prepared composite (Fig. 2e) confirmed the partial complexation process with the appearance of weak bands at 915 and 940 cm^{-1} which belong to the two cis doubly bonded oxygens at

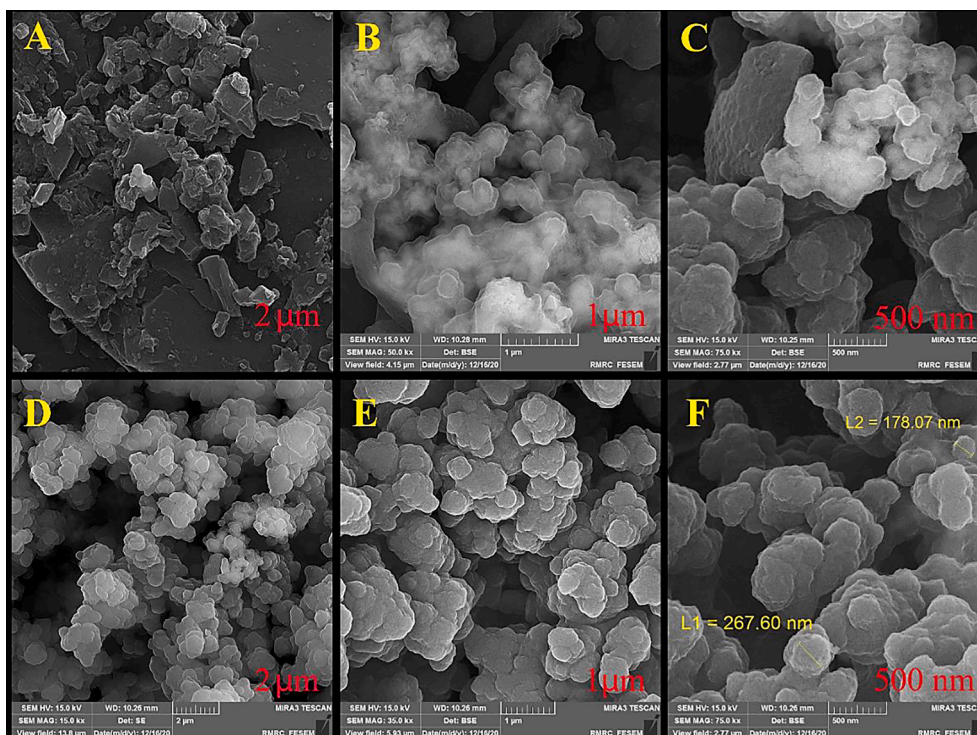


Fig. 6. FESEM photographs of Co_3O_4 @PPIL-Mo obtained under A-C) silent condition, and D-E) US irradiation.

the molybdenum core [36].

As can be seen, the peaks intensity of the determined catalyst was well prepared via ultrasonication (Fig. 3). The FT-IR spectra of US-treated samples exhibited a significant difference compared to classical heating method as explained in the following. According to the FT-IR spectra, conventional heating intense condition slightly damaged the structure of vinyl-modified Co_3O_4 NPs. The partial loading of MPS onto the Co_3O_4 NPs leads to weak peaks (Fig. 2). While, the polymerization process was done properly under US irradiation and as a result, the absorption band at 1550, which belonged to $\text{C}=\text{C}$ of MPS disappeared (Fig. 2d', e'). Two obvious peaks about $900\text{--}1020\text{ cm}^{-1}$ referred to the successful complexation process (Fig e').

The prepared composite under the US and reflux methods was investigated by the measurements of XRD analysis (Fig. 4). The XRD graph of the Co_3O_4 @PPIL-Mo clearly illustrated 7 diffraction angles (2θ)

at 31.70 , 37.26 , 38.97 , 45.17 , 56.11 , 59.77 , and 65.62 . The mentioned peaks that appeared were consistent with Co_3O_4 (JCPDS No. 01-080-1533, fcc, Fd3m) [37]. A broad peak about $2\theta = 22^\circ$ is attributed to the amorphous Si [38]. However, no diffraction peak characteristic of molybdenum was recorded which can be owing to its poor crystallinity and low concentrations. In fact, XRD analysis, confirms that the Mo (VI) loading retains the main crystalline structure of prepared catalyst [39]. The diffractograms revealed the presence of spinel structure in both methods and the graphs were the same.

Qualitative analysis of the porosity and specific surface area was determined by nitrogen sorption experiments (Fig. 5). It can be seen that the ultrasound-treated sample is typical IV isotherm with an obvious H1 type hysteresis shape, implying the presence of micro-pores (Fig. 5A). Moreover, as demonstrated in Fig. 5B, the sample of Co_3O_4 @PPIL-Mo illustrated the isotherm of type IV with a distinctive H2 type hysteresis

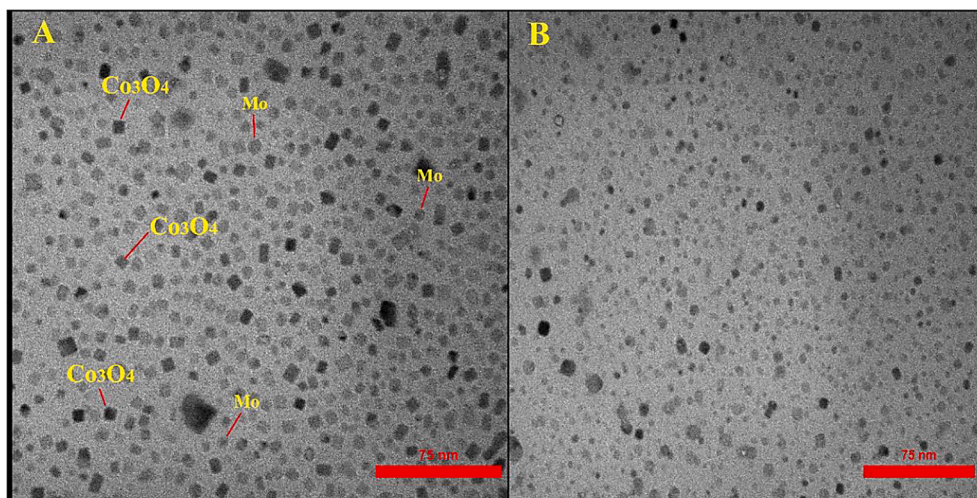


Fig. 7. TEM images of the as-prepared Co_3O_4 @PPIL-Mo obtained under A) US, and B) reflux, conditions.

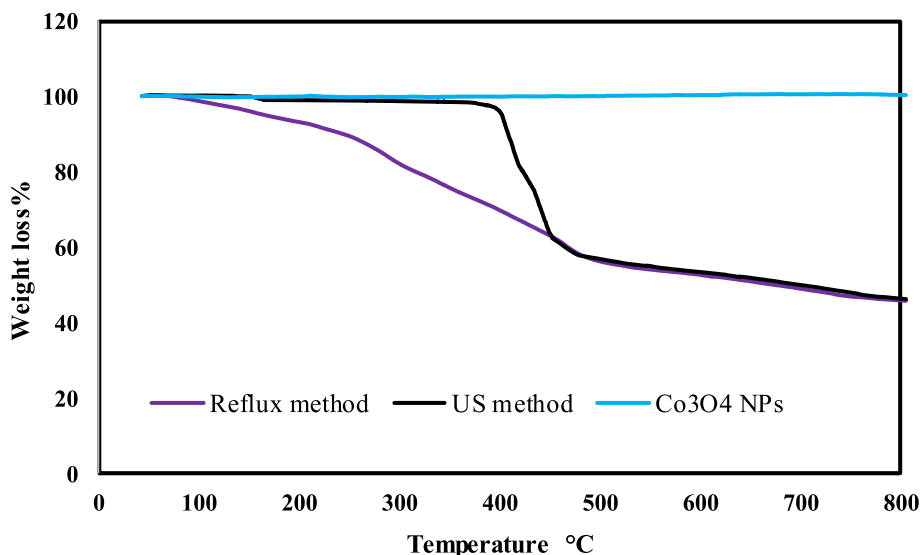


Fig. 8. TGA curves of pure Co₃O₄ NPs, and Co₃O₄@PPIL-Mo obtained via two different methods.

loop, revealing the existence of *meso*-porosity under reflux condition. The crosslinking poly ionic liquid was synthesized via ultrasonic agitation, and demonstrated well-defined pore channels with a higher surface area (223.83 m²/g) and larger pore volume (0.27 cm³/g) compared to the sample prepared in reflux condition (disordered pores with surface area 79.19 m²/g and 0.21 m³/g pore volume). The pore size distribution curves (Fig. 5C) further revealed that the pore size distribution was centered at 7 nm and 12–13 nm under reflux condition. While, the ultrasound-treated sample provides the pore size distribution about 3–4 nm. Generally, the interaction between polymer chains can be controlled by the pore structures. Intense shock waves of US radiations can be employed as micro liquid jets that modify the surface of the polymer, and the porous and cavities regions can be increased accordingly. With ultrasonic treatment, the breakup of agglomerates led to the increase in specific surface area (active sites).

The TEM and FESEM were used to study the morphology, uniformity and size of the produced PPIL via different protocols. As it can be seen in (Fig. 6D-F), an obvious cross-linked polymeric network including metallic core and poly ionic liquid was formed under US irradiation. The average size of particles was estimated via Digimizer software to be about 200 nm. Ultrasound irradiation provides definite cross-linked spherical shapes without any agglomeration. The results reveal that sonochemistry has widely acted as an initiator to enhance the polymerization rate for the preparation of PPILs. In contrast, the agglomerated particles are formed under classical heating (Fig. 6B, C). In addition, it is properly not cross-linked under silent condition (Fig. 6A). This occurs owing to lack of proper physico-mechanical force for the dispersion process. The TEM images of the samples with non-ultrasonic and ultrasonic treatments in water are shown in (Fig. 7. A, B). It is observable on the TEM image (7A) that the use of ultrasound promotes

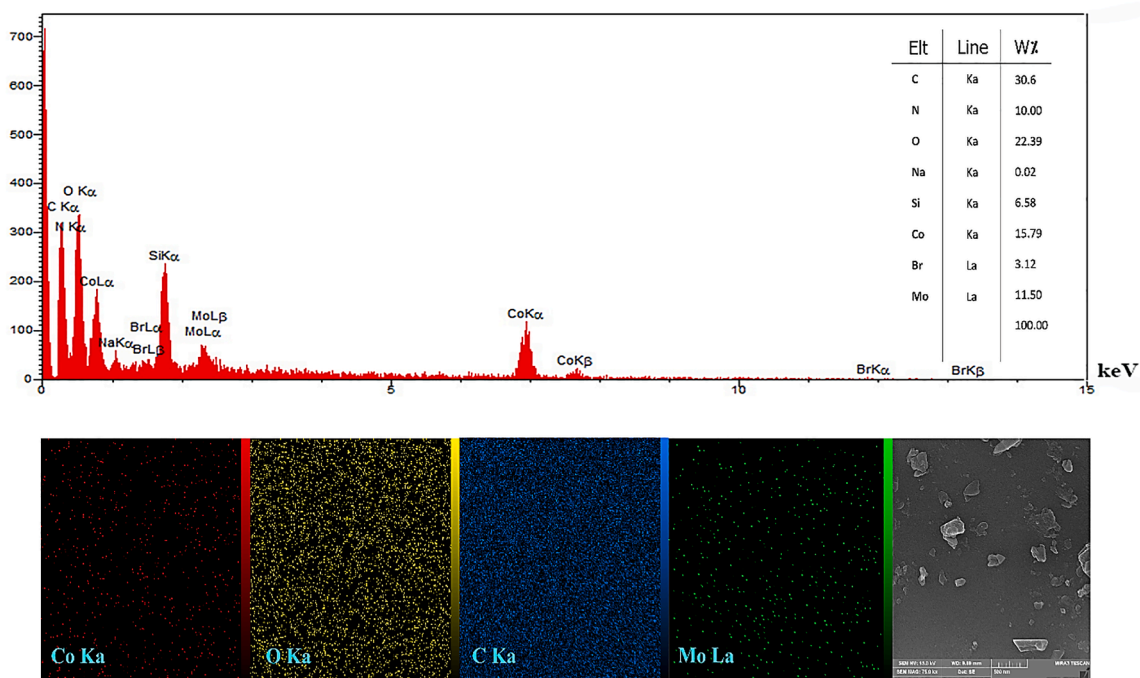


Fig. 9. EDX analysis and elemental mapping images of proposed catalyst.

Table 2
Optimization of the reaction conditions for the synthesis of **5a** by Co_3O_4 @PPIL-Mo.



Entry	Solvent	Catalyst	Condition	Time (min)	Yield ^b %
1	H ₂ O	–	US	20	18
2	H ₂ O	Co ₃ O ₄ NPs (10 mol%)	US	5	68
3	H ₂ O	Co ₃ O ₄ @PPIL (10 mol %)	US	5	87
4	H ₂ O	IL	US	5	73
5	H ₂ O	Co ₃ O ₄ @PPIL-Mo (10 mol%)	US	5	91
6	H ₂ O	Co ₃ O ₄ @PPIL-Mo (10 mol%)	US	5	98
7	H ₂ O	Co ₃ O ₄ @PPIL-Mo (5 mol%)	US	5	82
8	H ₂ O	Co ₃ O ₄ @PPIL-Mo (15 mol%)	US	5	98
9	H ₂ O	Co ₃ O ₄ @PPIL-Mo (10 mol%)	Δ	90	96
10	EtOH	Co ₃ O ₄ @PPIL-Mo (10 mol%)	US	10	93
11	EtOH/H ₂ O	Co ₃ O ₄ @PPIL-Mo (10 mol%)	US	10	95
12	CH ₃ CN	Co ₃ O ₄ @PPIL-Mo (10 mol%)	US	10	90
13	MeOH	Co ₃ O ₄ @PPIL-Mo (10 mol%)	US	10	91
14	DMF	Co ₃ O ₄ @PPIL-Mo (10 mol%)	US	20	62
15	Dioxane	Co ₃ O ₄ @PPIL-Mo (10 mol%)	US	20	55
16	H ₂ O	Co ₃ O ₄ @PPIL-Mo (10 mol%)	US 20 kHz	5	88
17	H ₂ O	Co ₃ O ₄ @PPIL-Mo (10 mol%)	US 60 kHz	5	98

^aReaction conditions: isatin (1 mmol), DMAD (1 mmol), malononitrile (1 mmol), and hydrazine hydrate (1 mmol) under US irradiation (40 KHz, 100 W).

^bIsolated yields.

the synthesis of composite to regular cubic (Co_3O_4 NPs in accordance with XRD patterns) and spherical shapes (molybdenum moieties) with uniform sizes. The TEM image (6B) reveals that the prepared catalyst mostly resulted in irregular shapes and sizes in silent condition.

Thermogravimetric analysis (TGA) of the Co_3O_4 @PPIL-Mo was investigated to determine the US radiation effect on thermal stability. The loss of weight at low temperature (<200 °C) in the beginning is related to the evaporation of physical adsorb water because of the hydrophilic nature of ionic liquid units (Fig. 8). The onset thermal degradation temperature (T_d) values for the US and reflux methods were about 400 and 248 °C, respectively. Maximal peak shift towards higher temperature is also related to the more thermal stability of the ultrasound-treated sample. The Co_3O_4 @PPIL-Mo which was obtained using the US method revealed a 50.24% weight loss between 400 °C and 476 °C; and this can be because of the decomposition of the main bond between ionic monomers and crosslinking. TGA curve also reveals that Co_3O_4 @PPIL-Mo composite is basically stable up to about 248 °C under reflux condition. These observations indicate that ultrasound irradiation has a significant treatment effect on the thermal stability of the proposed catalyst which can definitely fit to the synthesis of spiro-pyranopyrazole derivatives. It is assumed, well cross-linked structure leads to high thermal stability of US-treated sample.

EDX analysis of proposed catalyst is indicated in (Fig. 9). All lines are allocated to C, O, N, Co, Mo, Si, and Br elements for US-treated sample. The percentage of elements are demonstrated in Fig. 9. Furthermore, elemental mapping images clearly revealed that all elements are well distributed throughout the Co_3O_4 @PPIL-Mo slices (Fig. 9).

3.2. Application of ultrasound-treated Co_3O_4 @PPIL-Mo catalyst for the regioselective synthesis of mono-spiro derivatives and synergistic catalysis effect

The one-pot multicomponent reaction between isatin, dimethyl acetylenedicarboxylate (DMAD), malononitrile, and hydrazine hydrate was primarily selected as a model reaction to observe the catalytic

activity of the prepared Co_3O_4 @PPIL-Mo. Different conditions utilized to optimize the reaction and empirical results are mentioned in (Table 2). At first, H₂O was chosen as the greenest solvent to perform the model reaction in the presence of various catalysts. According to the data, conducting a reaction without any catalyst led to the trace yield (entry 1). Based on the experimental results, in spite of the fact that the Co_3O_4 @PPIL-Mo prepared under traditional heating was more effective (Table 2, entry 5), the ultrasound-treated composite could be considered the optimal one (Table 2, entry 6). Moreover, the remarkable effect of ultrasound on the structural and textural attributes (such as porosity, surface area, etc.) resulted in better performance of the proposed catalyst. An extensive set of experiments were performed to regulate the catalyst amount. In this regard, the yield was enhanced from 82 to 98% by enhancing the amount of Co_3O_4 @PPIL-Mo from 5 to 10 mol% while more catalyst did not increase the yield of the reaction (Table 2, entry 6,7,8). H₂O was selected as the solvent to conduct the reaction by mechanical stirring under silent condition and to specify the effect of ultrasonic agitation (Table 2, entry 9). The experimental results revealed that during a longer period, reaction yield is lower than sonication. As it can be hypothesized, there is a significant synergistic effect between US waves and active catalytic sites. From chemical aspect, the metal transition complex was integrated with the π conjugated system (including carbon-carbon double bond and N atom). Frequent irradiations of the US waves led to acceleration in the electronic transfer, and Mo complex changed to an activated site. Furthermore, collapse of cavitation bubbles supplied localized hot spots with great pressures that were in charge of the needed molecular fragmentation and bonding energy. Based on the physical point of view, catalyst dispersion in the media was facilitated in US irradiation and as a result, a greater surface area was created. All of these events can help the reaction to happen quickly. Thereafter, the influence of solvents was explored. Moreover, methanol, ethanol, and acetonitrile generate medium yields in longer times (Table 2, entries 10, 12, and 13). The product yields were also about 55% and 62% while the reaction was conducted in dioxane and DMF, respectively. According to the obtained result, H₂O can be considered an optimal solvent for

Table 3
Synthesis of spiroprano[2,3-c]pyrazole carboxylate derivatives under ultrasound and MW irradiations ^a.

Entry	X	R	Product	Time (min)	Yield ^b (%)	mp (°C)	lit.mp (°C)
1	5-H	H	5a	US	5	98	267–269
				MW	15	97	268 ^[42]
2	5-Cl	H	5b	US	7	98	293
				MW	20	95	293–295 ^[42]
3	5-Br	H	5c	US	5	97	>300
				MW	20	96	>300
4	5-Me	H	5d	US	7	97	>300
				MW	25	93	304–305 ^[42]
5	5-OMe	H	5e	US	8	92	253–254
				MW	40	90	251–253 ^[42]
6	5,7-Cl	H	5f	US	10	91	>300
				MW	45	88	NEW
7	H	Ph	5 g	US	10	92	272
				MW	45	89	270–271 ^[42]
8	5-Cl	Ph	5 h	US	10	90	261–263
				MW	50	85	262–264 ^[13]
9	5-Br	Ph	5i	US	6	94	258
				MW	30	90	258–260 ^[42]
10	5-Me	Ph	5j	US	8	95	258
				MW	40	90	255–257 ^[42]
11 12	5-OMe 5,7-Cl	Ph Ph	5 k 5 l	US	6	94	272 > 300
				MW	25	85	270–272 ^[13] NEW
MW 45				US	10	80	
						85	
					78	94	

^a Reaction conditions: US-treated Co₃O₄@PPIL-Mo (10 mol%) in water under US irradiation (40 KHz, 100 W) or MW (200 W).

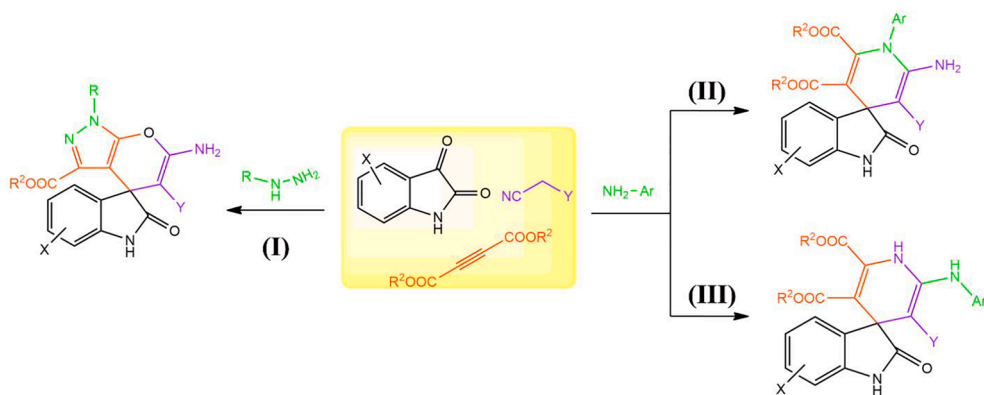
^b Isolated yields.

Table 4
Synthesis of spiro[indoline-3,4'-pyridine] derivatives under ultrasound and MW irradiations ^a.

Entry	X	Ar	Product	Time (min)	Yield ^b (%)	mp (°C)	lit.mp (°C)
1	H	C ₆ H ₅	6a	US	10	90	224–226
				MW	30	88	225–226 ^[48]
2	H	4-BrC ₆ H ₄	6b	US	12	88	293
				MW	30	85	290–292 ^[48]
3	H	4-OCH ₃ C ₆ H ₄	6c	US	8	92	255–257
				MW	20	89	>250 ^[48]
4	H	4-CH ₃ C ₆ H ₄	6d	US	10	89	253–254
				MW	25	83	>250 ^[48]
5	Cl	4-OCH ₃ C ₆ H ₄	6e	US	5	92	270
				MW	20	90	270–272 ^[48]
6	Cl	4-CH ₃ C ₆ H ₄	6f	US	9	91	234
				MW	30	88	232–234 ^[48]

^aReaction conditions: US-treated Co₃O₄@PPIL-Mo (10 mol%) in water under US irradiation (40 KHz, 100 W) or MW (200 W).

^bIsolated yields.

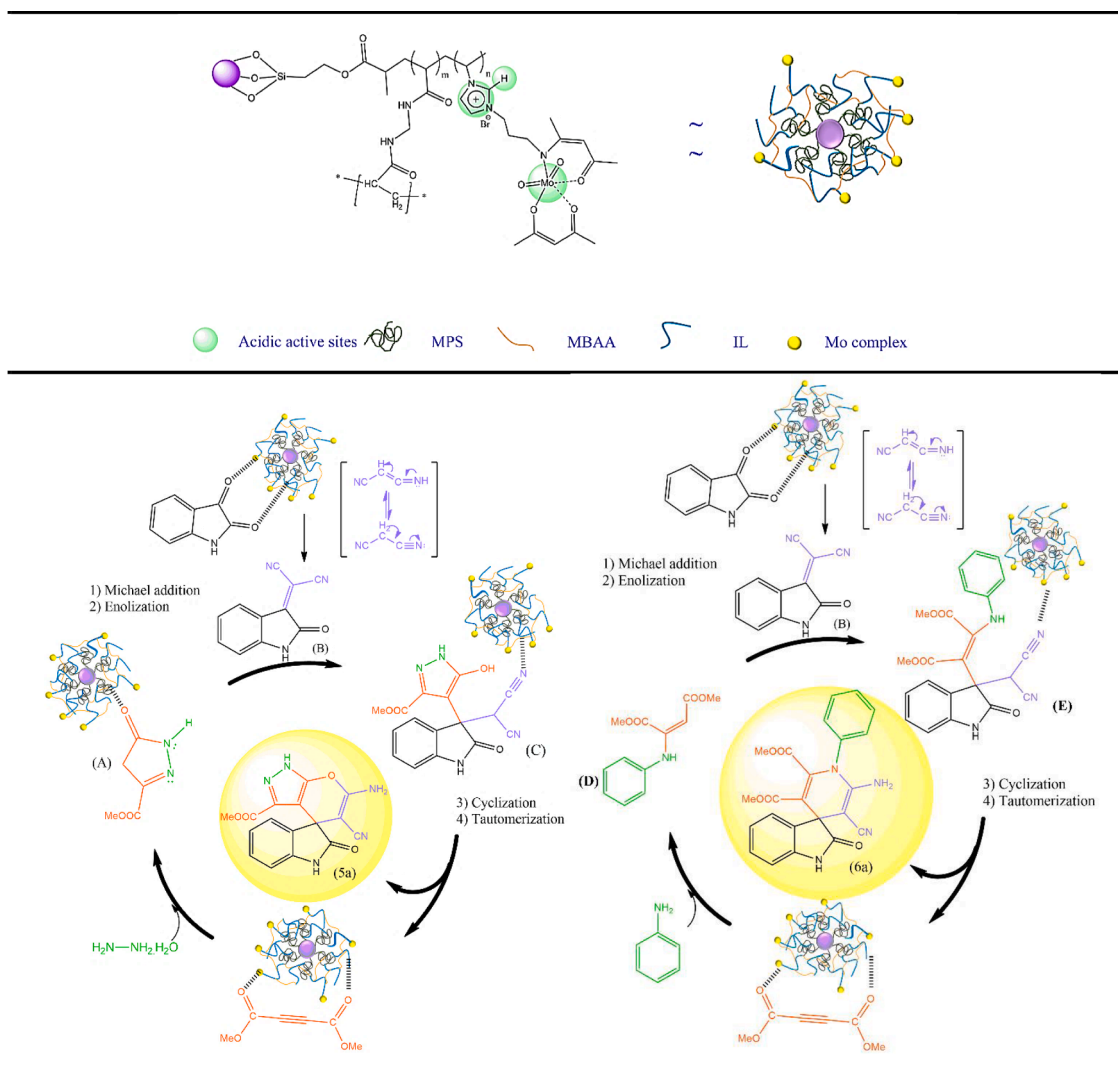


Scheme 2. Four-component reaction of isatins, active methylene, DMAD, and different amine components.

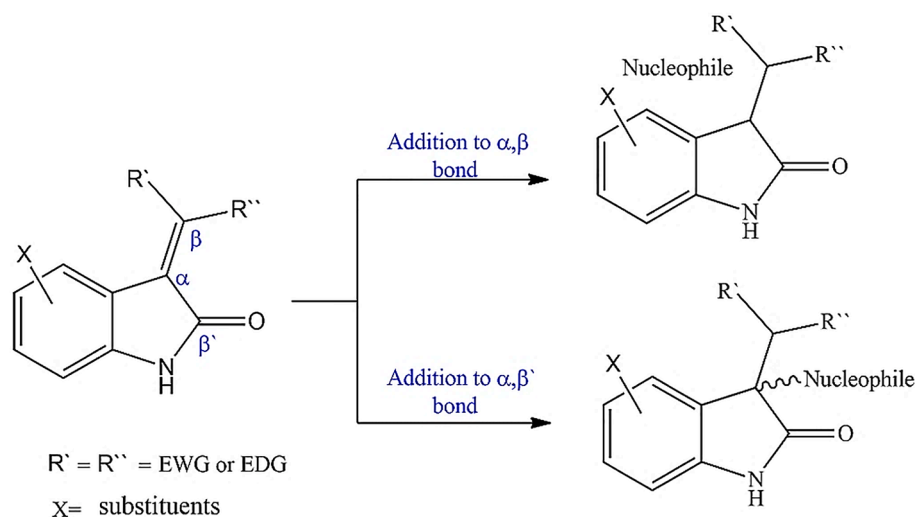
preparing 5a. This is because the polar intermediate has formed during the reaction. Finally, in order to check the irradiation frequency effect, the reaction was done in 20, 40, and 60 kHz (100 W). When the frequency irradiation increased from 20 kHz to 40 kHz, the yield of 5a changed significantly (from 88% to 98%) (Table 2, entry 6,16). However, increasing the irradiation frequency from 40 to 60 kHz (Table 2, entry 17) did not have a considerable effect on the yield of 5a (98% in a

similar time). Therefore, the use of the ultrasound-treated $\text{Co}_3\text{O}_4@\text{PPIL-Mo}$ catalyst (10 mol%) in H_2O under US agitation can be introduced as the optimal reaction condition (40 kHz, 100 W).

Subsequently, to demonstrate the scope and applicability of this catalyst in the one-pot four-component synthesis of spiropranopyrazole derivatives, the reaction was extended to other isatins which were replaced. These findings clearly demonstrated that this catalytic



Scheme 3. The plausible mechanisms for one-pot synthesis of 5a and 6a.



Scheme 4. Preparation of regioisomers through conjugate nucleophile addition.

procedure can be extended to many different substrates in order to make a variety-oriented library of spiropyranopyrazoles (Table 3). The electronic structure of the substituents (C5 of isatins) could also be possible with high yields. This straightforward approach was extended in a series, using phenyl hydrazine instead of hydrazine hydrate component, which formed the desired spiro pyranopyrazole derivatives in excellent yield. We found that reactions with hydrazine hydrate could afford the desired products within shorter times because of its low steric hindrance [13]. Furthermore, to gain more insight into the effect of US on the synthetic pathway, the reactions were performed under two green protocols including microwave (MW) and ultrasound (US) irradiations without any undesirable byproducts in good to excellent yields and short reaction times. Clearly, US waves were found to have a remarkable effect on the preparation of spiro pyranopyrazoles, indicating its superiority over the MW method with respect to the yields and reaction times. Ultrasonic phenomena improve heterogeneous reaction rates through increasing the mixing between reactants, controlling the distribution of particles, accelerating the diffusion of products and reactants, and promoting the generation of a new solid phase [40]. It is remarkable that MW-accelerated chemical reactions depend on the capacity mixture to absorb MW energy. This capacity also depends on some main factors such as the polarity of reactants or intermediates and the nature of solvents [41].

To further widen the reaction scope, we tried to apply aromatic amines to replace hydrazines. Encouraging results were achieved, another multicomponent reaction was obtained and a different scaffold was produced. According to the obtained results, a library of spiro1,4-dihydropyridines has been synthesized in good yields with no change in the optimized conditions (Table 4). Under the same conditions, various amine components (aromatic amine and hydrazine derivatives) afford different product skeletons (Scheme 2). In fact, some parameters such as the electronic and steric qualities of substituents, nature of catalyst, etc. can influence the main product of reactions. For example, a one-pot four-component reaction of isatin, DMAD, malononitrile, and aromatic amines using different iodine sources as catalyst selects rout (III) [43] While the same four-component reaction in the presence of Dabco-based IL crosses rout (II) [13].

On the basis of our previous successful studies on the synthesis of heterocyclic compounds using various catalysts [44–46], the proposed reaction pathway mechanism for the synthesis of 5a is shown in (Scheme 3). At first, the catalyst facilitated Knoevenagel condensation of isatin and malononitrile for the formation of adduct B (isatylidene malononitrile) through different acidic sites which react with adduct A (pyrazolone) generated through the condensation of hydrazine hydrate and

Table 5
Comparative study between reported catalyst and US-treated $\text{Co}_3\text{O}_4@PPIL\text{-Mo}$.

Product	Catalyst ^{Ref.}	Condition	Yield%	Time
5a	[Dabco-H][AcO] ¹³	EtOH/40 °C	96	30 min
	PEG-400 ⁴²	110 °C	86	3 h
	$\text{Co}_3\text{O}_4@PPIL\text{-Mo}$	US/ H_2O	98	5 min
6b	[Dabco-H][AcO] ¹³	EtOH/40 °C	86	4 h
	$\text{N}(\text{Et})_3$ ⁴⁸	EtOH/25 °C	83	24 h
	$\text{Co}_3\text{O}_4@PPIL\text{-Mo}$	US/ H_2O	90	10 min

dialkyl acetylene dicarboxylate in a regioselective manner. Ultrasound-treated catalyst provides favorable interactions between the imidazolium rings and the carbonyl groups. Apart from that, coordinated $\text{Co}_3\text{O}_4@PPIL\text{-Mo}$ to the carbonyl groups through Lewis acidic sites (Mo^{6+}) decreases the energy of transition state for the nucleophilic attack of the isatin to malononitrile (and hydrazine to DMAD). Michael addition of intermediate (A) onto isatylidene malononitrile followed by enolization provided adduct C. In the following, the hydroxyl group underwent fast nucleophilic addition to the CN moiety (intramolecular cyclization) and product 5a was obtained after tautomerization. On the whole, the asymmetric collapse form of micro liquid jet with high speed intensified the heat and accelerated the mass transfer among the pores and within the stationary film that was around the adsorbent [47]. These liquid jets made the heterogeneous catalyst active and the mass transfer better by disrupting the interfacial boundary layers. As an interesting point, the ultrasound also accelerated the deprotonation of malononitrile and hydrazine as well as the thermal deprotonation. As a result, the malononitrile and hydrazine anions were formed rapidly (Scheme 3).

With the catalyst activation by US agitations, the aniline adds on DMAD to afford the intermediate D (β -enamino ester) which undergoes addition with isatylidene malononitrile B to generate intermediate E. In the following, the amino group underwent fast nucleophilic addition to the CN moiety (intramolecular nucleophilic cyclization) and product 6a was obtained after tautomerization (Scheme 4).

It is worth mentioning that the generation of isatylidenemalononitrile (B) is noticed on thin layer chromatography, and the reaction regioselectivity is controlled by the relations between stereo-electronic factors of R' and R'' and the carbonyl of the 2-oxindole scaffold. Addition of pyrazolone or β -enamino ester (D) onto intermediate (B) was carried out through addition to α,β' bond in the presence of electron withdrawing groups (EWG) ($R',R'' = \text{CN}$). Among mentioned regioselective mechanism, US strategy also leads to improvement selectivity in organic transformations [49].

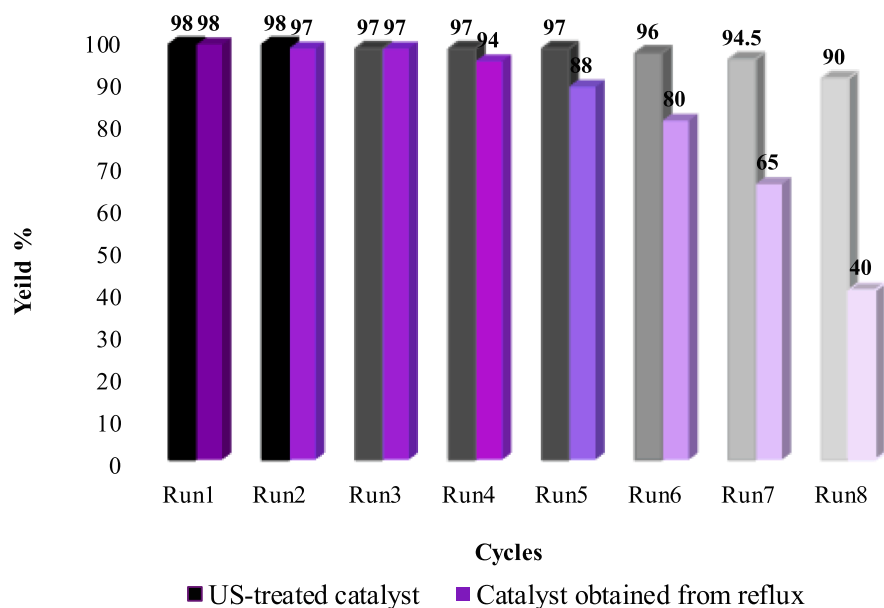


Fig. 10. Recyclability of Co_3O_4 @PPIL-Mo obtained from two different conditions.

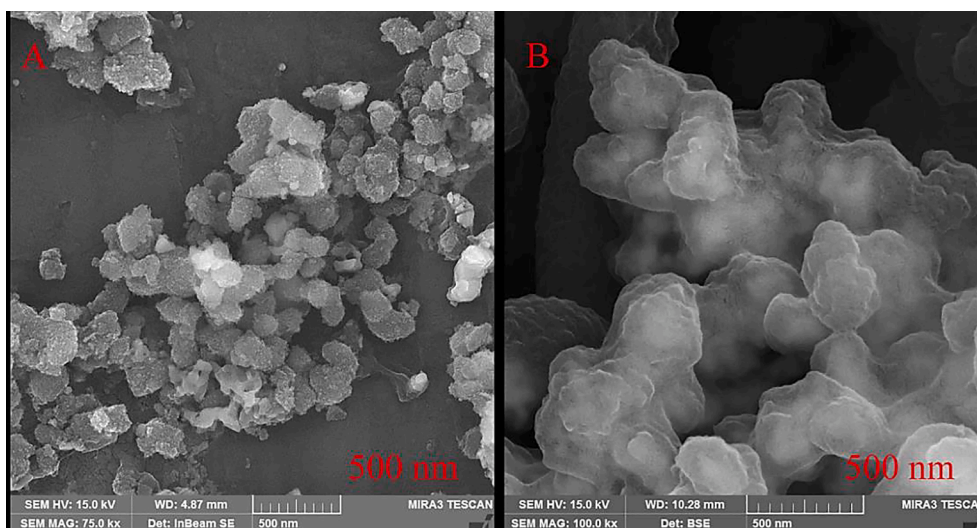


Fig. 11. FESEM images of the recovered Co_3O_4 @PPIL-Mo obtained from A) reflux, and B) US conditions.

A comparative investigation was carried out between synthesized Co_3O_4 @PPIL-Mo and reported catalyst for the preparation of spiro 1,4-dihydropyridines and spiro pyranopyrazoles. The results were summarized in Table 5. Ultrasound irradiation differs from conventional energy sources (such as heat, light, or ionizing radiation) in time, pressure, and energy per molecule. The US radiation in the presence of Co_3O_4 @PPIL-Mo composite provided highest reaction yield and shortest times in H_2O at room temperature.

Reusability is known as key characteristic properties of catalysts. Hence, the prepared catalyst was separated at the end of the reaction by centrifugation. The recovered catalyst was washed several times with EtOH and H_2O , dried overnight, and reused with fresh substrates. The outcomes indicated that the ultrasound-treated Co_3O_4 @PPIL-Mo could be reused eight cycles with no significant loss in its activity (Fig. 10).

Similarly, recoverability of Co_3O_4 @PPIL-Mo obtained under silent condition was also performed and found to have the ability to be reused for five cycles. The morphology of recovered catalyst after eight cycles was considered by FESEM (Fig. 11). The outcomes confirmed that the US-treated catalyst structure showed no significant change after

recovery (Fig. 11B). While, the cross-linked network of Co_3O_4 @PPIL-Mo obtained under silent condition completely disrupted and irregular shape particles obtained (Fig. 11A).

4. Conclusions

In conclusion, novel-supported molybdenum complex on cross-linked poly ionic liquid entrapped cobalt oxide nanoparticles was well fabricated via two different methods including ultrasound irradiations and reflux. The positive impact of ultrasound irradiations on the physicochemical properties (thermal stability, porosity, particle uniformity, reusability, and catalytic activity) of the catalyst was approved through the results of different characterization techniques. Furthermore, ultrasound radiation caused great dispersion of Co_3O_4 NPs, perfect surfaces functionalization, enhanced polymerization rate, and uniform distribution of Mo (VI) Schiff-base complexes on the polymeric networks. Accordingly, US-treated Co_3O_4 @PPIL-Mo introduced as a potentially strong heterogeneous catalyst for the four-component synthesis of spiro 1,4-dihydropyridines and spiro pyranopyrazoles. US wave

radiations were found to have a beneficial effect on the regioselective synthesis of mono-spiro compounds, indicating their superiority over the MW method with respect to the yields and reaction times. The features of ultrasound-assisted organic transformations; namely, the regioselectivity, ease of experimental manipulation, and enhanced reaction rates are highlighted in this work.

CRedit authorship contribution statement

Zahra Elyasi: Conceptualization, Data curation, Software, Writing - original draft. **Javad Safaei Ghomi:** Methodology, Supervision, Writing - review & editing. **Gholam Reza Najafi:** Data curation, Investigation, Validation, Visualization.

Declaration of Competing Interest

The authors declare that they have no known competing financial interests or personal relationships that could have appeared to influence the work reported in this paper.

Acknowledgments

The authors acknowledge a reviewer who provided helpful insights. The authors are grateful to the Islamic Azad University, Qom Branch, Qom, I. R. Iran for supporting this work.

Appendix A. Supplementary data

Supplementary data to this article can be found online at <https://doi.org/10.1016/j.ulsonch.2021.105614>.

References

- [1] T.G. Mckenzie, F. Karimi, M. Ashokkumar, G.G. Qiao, *Ultrasound and Sonochemistry for Radical Polymerization: Sound Synthesis*, *Chem. Eur. J.* 25 (2019) 5372–5388.
- [2] S. Afreen, K. Muthoosamy, S. Manickam, *Sono-nano chemistry: A new era of synthesising polyhydroxylated carbon nanomaterials with hydroxyl groups and their industrial aspects*, *Ultrason. Sonochem.* 51 (2019) 451–461.
- [3] W. Cai, T. Hu, A.M. Bakry, Z. Zheng, Y. Xiao, Q. Huang, *Effect of ultrasound on size, morphology, stability and antioxidant activity of selenium nanoparticles dispersed by a hyperbranched polysaccharide from *Lignosus rhinocerotis**, *Ultrason. Sonochem.* 42 (2018) 823–831.
- [4] G. Chatel, *How sonochemistry contributes to green chemistry?* *Ultrason. Sonochem.* 40 (2018) 117–122.
- [5] F. Penteado, B. Monti, L. Sancineto, G. Perin, R.G. Jacob, C. Santi, E.J. Lenardão, *Ultrasound-assisted multicomponent reactions, organometallic and organochalcogen chemistry*, *Asian. J. Org. Chem.* 7 (12) (2018) 2368–2385.
- [6] L. Chen, J. He, *DABCO-Catalyzed Michael/Alkylation Cascade Reactions Involving α -Substituted Ammonium Ylides for the Construction of Spirocyclopropyl Oxindoles: Access to the Powerful Chemical Leads against HIV-1*, *J. Org. Chem.* 85 (2020) 5203–5219.
- [7] P. Ferreira-Chamorro, A. Redondo, G. Riego, O. Pol, *Treatment with 5-fluoro-2-oxindole Increases the Antinociceptive Effects of Morphine and Inhibits Neuropathic Pain*, *Cell. Mol. Neurobiol.* (2020), <https://doi.org/10.1007/s10571-020-00952-w>.
- [8] P. Dhokne, A.P. Sakla, N. Shankaraiah, *Structural Insights of Oxindole based Kinase Inhibitors as Anticancer Agents: Recent Advances*, *Eur. J. Med. Chem.* 216 (2021) 113334, <https://doi.org/10.1016/j.ejmech.2021.113334>.
- [9] S. Sampath, M. Vadivelu, R. Ravindran, P.T. Perumal, V. Velkannan, K. Karthikeyan, *Synthesis of 1,2,3-Triazole Tethered 3-Hydroxy-2-oxindoles: Promising Corrosion Inhibitors for Steel in Acidic Medium and Their Anti-Microbial Evaluation*, *ChemistrySelect* 5 (2020) 2130–2134.
- [10] B.P. Kaur, J. Kaur, S. Singh Chimni, *Arenesulfonyl indole: new precursor for diversification of C-3 functionalized indoles*, *RSC Adv.* 11 (2021) 2126–2140.
- [11] A. Toumi, S. Boudriga, K. Hamden, M. Sobeh, M. Cheurfa, M. Askri, M. Knorr, C. Strohmman, L. Brieger, *Synthesis, antidiabetic activity and molecular docking study of rhodaninesubstituted spirooxindole pyrrolidine derivatives as novel α -amylase inhibitors*, *Bioorg. Chem.* 106 (2020), 104507.
- [12] D.M. Pore, P.B. Patil, D.S. Gaikwad, P.G. Hegade, J.D. Patil, K.A. Undale, *Green access to novel spiro pyranopyrazole derivatives*, *Tetrahedron Lett.* 54 (44) (2013) 5876–5878.
- [13] T. Liu, Y.H. Lai, Y.Q. Yu, D.Z. Xua, *A facile and efficient procedure for one-pot four-component synthesis of polysubstituted spiro pyrano[2,3-c]pyrazole and spiro 1,4-dihydropyridine catalyzed by Dabco-based ionic liquid under mild condition*, *New J. Chem.* 42 (2018) 1046–1051.
- [14] R.L. Vekariya, *A review of ionic liquids: Applications towards catalytic organic transformations*, *J. Mol. Liq.* 227 (2017) 44–60.
- [15] Z. Lei, B. Chen, Y.M. Koo, D.R. MacFarlane, *Introduction: Ionic Liquids*, *Chem. Rev.* 117 (2017) 6633–6635.
- [16] T. Welton, *Ionic liquids: a brief history*, *Biophys. Rev.* 10 (2018) 691–706.
- [17] H.-P. Steirück, P. Wasserscheid, *Ionic Liquids in Catalysis*, *Catal. Lett.* 145 (1) (2015) 380–397.
- [18] B. Karimi, M. Tavakolian, M. Akbari, F. Mansouri, *Ionic Liquids in Asymmetric Synthesis: An Overall View from Reaction Media to Supported Ionic Liquid Catalysis*, *ChemCatChem.* 10 (2018) 3173–3205.
- [19] S.-Y. Zhang, Q. Zhuang, M. Zhang, H. Wang, Z. Gao, J.-K. Sun, J. Yuan, *Poly(ionic liquid) composites*, *Chem. Soc. Rev.* 49 (6) (2020) 1726–1755.
- [20] W. Qian, J. Texter, F. Yan, *Frontiers in poly(ionic liquid)s: syntheses and applications*, *Chem. Soc. Rev.* 46 (2017) 1124–1159.
- [21] A. Zaoui, Z. Cherifi, M. Belbachir, *Ultrasound-induced synthesis of an imidazolium based poly(ionic liquid) in an aqueous media: A structural, thermal and morphological study*, *Ultrason. Sonochem.* 55 (2019) 149–156.
- [22] R. Sumitani, T. Mochida, *Metal-Containing Poly(ionic liquid) Exhibiting Photogeneration of Coordination Network: Reversible Control of Viscoelasticity and Ionic Conductivity*, *Macromolecules* 53 (2020) 6968–6974.
- [23] T. Yamamoto, K. Kawaguchi, Y. Takahashi, *Particle size control in the soap-free emulsion polymerization of styrene by an oil-soluble initiator with a weakly acidic water-soluble initiator*, *Colloids Surf. A Physicochem. Eng. Asp.* 502 (2016) 1–5.
- [24] T. Yamamoto, K. Kawaguchi, *Relationship between surface potential and particle size in soap-free emulsion copolymerization of styrene and methyl methacrylate using a water- or oil-soluble initiator*, *Colloid Polym. Sci.* 294 (2016) 281–284.
- [25] C. Imberti, P. Zhang, H. Huang, P.J. Sadler, *New designs for phototherapeutic transition metal complexes*, *Angew. Chem. Int. Ed.* 132 (1) (2020) 61–73.
- [26] C. Wei, Y. He, X. Shi, Z. Song, *Terpyridine-metal complexes: Applications in catalysis and supramolecular chemistry*, *Coord. Chem. Rev.* 385 (2019) 1–19.
- [27] F. Glaser, O.S. Wenger, *Recent progress in the development of transition-metal based photoredox catalysts*, *Coord. Chem. Rev.* 405 (2020), 213129.
- [28] M.A. Ghasemzade, M.H. Abdollahi-Basir, Z. Elyasi, *Synthesis of Some Novel Imidazoles Catalyzed by Co_3O_4 Nanoparticles and Evaluation of their Antibacterial Activities*, *Comb. Chem. High Throughput Screen.* 21 (2018) 271–280.
- [29] Z. Elyasi, J. Safaei Ghomi, G.R. Najafi, M.R. Zand Monfared, *Zand Monfared, The influence of the polymerization approach on the catalytic performance of novel porous poly (ionic liquid)s for green synthesis of pharmaceutical spiro-4-thiazolidinones*, *RSC Adv.* 10 (72) (2020) 44159–44170.
- [30] S. Salatin, S. Maleki Dizaj, A. Yari Khosroushahi, *Effect of the surface modification, size, and shape on cellular uptake of nanoparticles*, *Cell Biol. Int.* 39 (8) (2015) 881–890.
- [31] G. Liu, M. Hou, J. Song, T. Jiang, H. Fan, Z. Zhang, B. Han, *Immobilization of Pd nanoparticles with functional ionic liquid grafted onto cross-linked polymer for solvent-free Heck reaction*, *Green Chem.* 12 (1) (2010) 65–69.
- [32] A. Pourjavadi, S.H. Hosseini, N. Zohrehb, C. Bennette, *Magnetic Nanoparticle Entrapped into the Cross-linked Poly(imidazole/imidazolium) Immobilized Cu(II): An Effective Heterogeneous Copper Catalyst*, *RSC Adv.* 4 (2014) 46418–46426.
- [33] M. Zhang, Y.H. Liu, Z.R. Shang, H.C. Hu, Z.H. Zhang, *Supported molybdenum on graphene oxide/ Fe_3O_4 : An efficient magnetically separable catalyst for one-pot construction of spiro-oxindole dihydropyridines in deep eutectic solvent under microwave irradiation*, *Catal. Commun.* 88 (2017) 39–44.
- [34] M. Hassanpour, H. Safardoust-Hojaghan, M. Salavati-Niasari, *Degradation of methylene blue and Rhodamine B as water pollutants via green synthesized $\text{Co}_3\text{O}_4/\text{ZnO}$ nanocomposite*, *J. Mol. Liq.* 229 (2017) 293–299.
- [35] V. Thangaraj, A. Bhaskarapillai, S. Velmurugan, *Synthesis of a crosslinked poly (ionic liquid) and evaluation of its antimony binding properties*, *J. Hazard. Mater.* 384 (2020), 121481.
- [36] M. Bagherzadeh, M. Balali, M.M. Haghdoost, H. Keypour, *Synthesis and characterization of molybdenum complex supported on magnetic and non-magnetic supports: comparing their catalytic activity, selectivity, and reusability*, *J. Iran. Chem. Soc.* 16 (2019) 673–685.
- [37] R.C. Xie, M. Volokhova, A. Boldin, L. Seiberg, M. Tsujimoto, M. Yang, B. Rasche, R.G. Compton, *Electro-catalytic oxidation of hydroxide ion by Co_3O_4 and $\text{Co}_2\text{O}_3/\text{SiO}_2$ nanoparticles both at particle ensembles and single particle level*, *ChemElectroChem.* 7 (2020) 1261–1276.
- [38] R. Taheri-Ledari, J. Rahimi, A. Maleki, *Synergistic catalytic effect between ultrasound waves and pyrimidine-2,4-diamine-functionalized magnetic nanoparticles: Applied for synthesis of 1,4-dihydropyridine pharmaceutical derivatives*, *Ultrason. Sonochem.* 59 (2019) 104737, <https://doi.org/10.1016/j.ulsonch.2019.104737>.
- [39] J. Tang, W. Dong, G. Wang, Y. Yao, L. Cai, Y. Liu, X. Zhao, J. Xu, L. Tan, *Efficient molybdenum(VI) modified Zr-MOF catalysts for epoxidation of olefins*, *RSC Adv.* 4 (2014) 42977.
- [40] B. Banerjee, *Recent developments on ultrasound-assisted one-pot multicomponent synthesis of biologically relevant heterocycles*, *Ultrason. Sonochem.* 35 (2017) 15–35.
- [41] G. Chatel, R.S. Varma, *Ultrasound and microwave irradiation: contributions of alternative physicochemical activation methods to Green Chemistry*, *Green Chem.* 21 (2019) 6043.
- [42] K. Karnakar, K. Ramesh, K.H.V. Reddy, B.S.P. Anil Kumar, J.B. Nanubonula, Y.V. D. Nageswar, *A Novel One pot four-component reaction for the efficient synthesis of spiro[indoline-3,4'-pyrano[2,3-c]pyrazole]-3'-carboxylate and trifluoromethylated spiro[indole-3,4'-pyrano[2,3-c]pyrazole] derivatives using recyclable PEG-400*, *New J. Chem.* 39 (11) (2015) 8978–8983.

- [43] A. Mondal, B. Naskar, S. Goswami, C. Prodhon, K. Chaudhuri, C. Mukhopadhyay, I_2 catalyzed access of spiro[indoline-3,4'-pyridine] appended amine dyad: new ON-OFF chemosensors for Cu^{2+} and imaging in living cells, *Org. Biomol. Chem.* 16 (2018) 302.
- [44] J. Safaei Ghomi, Z. Akbarzadeh, Ultrasonic Accelerated Knoevenagel Condensation by Magnetically Recoverable $MgFe_2O_4$ Nanocatalyst: a Rapid and Green Synthesis of Coumarins under Solvent-Free Conditions, *Ultrason. Sonochem.* 40 (2018) 78–83.
- [45] J. Safaei Ghomi, S. Zahedi, Novel ionic liquid supported on Fe_3O_4 nanoparticles and its application as a catalyst in Mannich reaction under ultrasonic irradiation, *Ultrason. Sonochem.* 34 (2017) 916–923.
- [46] J. Safaei-Ghomi, Z. Elyasi, P. Babaei, N-doped graphene quantum dots modified with CuO (0D)/ZnO (1D) heterojunctions as a new nanocatalyst for the environmentally friendly one-pot synthesis of monospiro derivatives, *New J. Chem.* 45 (3) (2021) 1269–1277.
- [47] J. Safari, L. Javadian, Ultrasound assisted the green synthesis of 2-amino-4H-chromene derivatives catalyzed by Fe_3O_4 -functionalized nanoparticles with chitosan as a novel and reusable magnetic catalyst, *Ultrason. Sonochem.* 22 (2015) 341–348.
- [48] J. Sun, Q. Wu, L. Zhang, C. Yan, Efficient Synthesis of the Functionalized Spiro [indoline-3,4'-pyridine] via Four-component Reaction, *Chin. J. Chem.* 30 (7) (2012) 1548–1554.
- [49] M. Ganesh, M.P. Rao, Diastereoselective Reactions Involving b-Mono- and b,b'-Disubstituted Alkylidene Oxindoles: Pondering Alkene Geometry, *Asian J. Org. Chem.* 7 (2018) 285–313.